Published in final edited form as:
Angew Chem Int Ed Engl. 2012 November 5; 51(45): 11302–11305. doi:10.1002/anie.201205082.

Perfluorinated Aromatic Spacers for Sensitizing Eu(III) in Dinuclear Oligomers: Better than the Best by Chemical Design?**

Dr. Jean-François Lemonnier,
Department of Inorganic, Analytical and Applied Chemistry, University of Geneva, 30 quai E. Ansermet, CH-1211 Geneva 4 (Switzerland)

Ms. Lucille Babel,
Department of Inorganic, Analytical and Applied Chemistry, University of Geneva, 30 quai E. Ansermet, CH-1211 Geneva 4 (Switzerland)

Dr. Laure Guénée,
Laboratory of Crystallography, University of Geneva, 24 quai E. Ansermet, CH-1211 Geneva 4 (Switzerland)

Dr. Prasun Mukherjee,
Department of Chemistry, University of Pittsburgh, 219 Parkman Avenue, Pittsburgh, PA 15260, USA

Prof. Dr. David H. Waldeck,
Department of Chemistry, University of Pittsburgh, 219 Parkman Avenue, Pittsburgh, PA 15260, USA

Dr. Svetlana V. Eliseeva,
Centre de Biophysique Moléculaire, CNRS UPR 4301, Rue Charles Sadron, F-45071 Orléans Cedex 2 (France)

Prof. Dr. Stéphane Petoud, and
Centre de Biophysique Moléculaire, CNRS UPR 4301, Rue Charles Sadron, F-45071 Orléans Cedex 2 (France)

Prof. Dr. Claude Piguet
Department of Inorganic, Analytical and Applied Chemistry, University of Geneva, 30 quai E. Ansermet, CH-1211 Geneva 4 (Switzerland)

David H. Waldeck: dave@pitt.edu; Stéphane Petoud: stephane.petoud@cnrs-orleans.fr; Claude Piguet: claude.piguet@unige.ch

Keywords

Sensitization; Lanthanide; Intersystem crossing; Energy transfer; Quantum yield

The unique optical characteristics of lanthanide ions (Ln^{III}) have driven their use in a wide range of applications, however the efficiency of populating directly their electronic states is limited so that the creation of an antenna to capture energy and generate excited Ln^{III} ions is

**This work was supported through grants from the Swiss National Science Foundation, the National Institute of Health, via NIH grant R21-EB008257-01A1, the National Science Foundation (CHE-0718755), la Ligue contre le Cancer and the Institut National de la Santé et de la Recherche Médicale (INSERM). The work was carried out within the COST Actions D38 and CM1006.

Correspondence to: David H. Waldeck, dave@pitt.edu; Stéphane Petoud, stephane.petoud@cnrs-orleans.fr; Claude Piguet, claude.piguet@unige.ch.

§Supporting Information for this article is available on the WWW under http://www.angewandte.org.

broadly important. In this context, metal-organic frameworks, hybrid materials, and nanoparticles randomly doped with homo- or heterometallic mixtures of luminescent lanthanide cations, Ln^{III}, are intensively being investigated for engineering luminescent devices for bright white lighting, for upconversion, and as sensing agents.[1] Although the exact location of the various metals in the final material is crucial for dual ligand-centered/metal-centered emission,[1l,m] for upconversion[1g] and for directional light-conversion[2a] processes, the preparation of organized polymetallic 4f-4f oligomers and polymers remains rare and challenging.[2] A statistical mechanics (Ising model) analysis suggests that standard repulsive nearest neighbor intermetallic interactions operating in linear polymers with regularly spaced binding sites should provide the targeted ordered …-Ln^1-Ln^2-Ln^1-Ln^2-… microstates.[3,4] Pioneering work in this field has relied on the bulk electropolymerization of didentate 1,10-phenanthroline with thienyl spacers[5] and the acyclic diene metathesis of tridentate 2,6-bis(benzimidazol-2-yl)pyridine,[6] followed by reaction with Eu(β-diketonate)$_3$ or $Eu(NO_3)_3$ to yield red-emitting metallopolymers. A reliable exploitation of this concept for the development of luminescent materials, however, requires the efficient sensitization of the luminophore via the rational optimization of each photophysical step by using chemical tools.

As a first step toward this goal, the rigid segmental ligand strands **L1–L3**, made of two tridentate binding units separated by a rigid and electronically-tunable aromatic spacer, have been reacted with trivalent europium to give the dinuclear complexes [Eu_2(**L*k***)(hfac)$_6$] (Scheme 1).[7] The use of a simple method for deciphering the various contributions to the sensitization mechanism clearly showed that [Eu_2(**L3**)(hfac)$_6$] displayed the largest global emission quantum yield (Φ_{Eu}^{L} =0.206(7), eq. 1) because of an efficient **L3**→Eu energy transfer step ($\eta_{en.tr.}^{L\rightarrow Eu}$=0.47(14) eq. 3, see the dark grey histograms in Fig. 1).[7]

Theoretical considerations suggest that $\eta_{en.tr.}^{L\rightarrow Eu}$ could benefit from a shift of the **L**($^3\pi^*$) state to higher energy produced by the perfluorination of the central aromatic spacer in **L4** (Scheme 2).[8] Correspondingly, the expected decrease of k_{nr}^{F} and k_{nr}^{Eu}, and of the so-called π-conjugation length A_π (eq. 5)[9] in [Eu_2(**L4**)(hfac)$_6$],[7] should optimize both intersystem crossing efficiency (η_{ISC} = 0.6(1), eq. 2) and intrinsic Eu-centered quantum yield (Φ_{Eu}^{Eu}=0.76(2), eq. 4) that were previously measured in [Eu_2(**L3**)(hfac)$_6$] (dark grey histograms in Fig. 1). Note that

$$\Phi_{Eu}^{L}=\eta_{ISC}\cdot\eta_{en.tr.}^{L\rightarrow Eu}\cdot\Phi_{Eu}^{Eu} \quad (1)$$

$$\eta_{ISC}=\frac{k_{ISC}}{k_r^F+k_{nr}^F+k_{ISC}}=k_{ISC}\cdot\tau_L\left(^1\pi^*\right) \quad (2)$$

$$\eta_{en.tr.}^{L\rightarrow Eu}=\frac{2k_{en.tr.}^{Eu}}{k_r^P+k_{nr}^P+2k_{en.tr.}^{Eu}}=2k_{en.tr.}^{Eu}\cdot\tau_L^{Eu}\left(^3\pi^*\right) \quad (3)$$

$$\Phi_{Eu}^{Eu}=\frac{k_r^{Eu}}{k_r^{Eu}+k_{nr}^{Eu}}=k_r^{Eu}\cdot\tau_{Eu} \quad (4)$$

and

$$k_r^F = k_{nr}^F \cdot e^{A_\pi} \quad (5)$$

The centrosymmetrical perfluorinated ligand **L4** is obtained through two successive Pd-catalyzed Suzuki-Myaura cross coupling reactions (Scheme 2, Figs. S1–S2). Stoichiometric mixing of **L4** with [Ln(hfac)$_3$(diglyme)] (2.0 eq) in chloroform gives [Ln$_2$(**L4**)(hfac)$_6$] (Ln = Gd, Eu) with a 80% yield. Slow evaporation from concentrated acetonitrile/chloroform solutions provides X-ray quality prisms (Table S1) containing S-shaped centrosymmetrical neutral [Eu$_2$(**L4**)(hfac)$_6$] complexes, in which the Eu atoms are separated by 14.667(1) Å (Fig. 2). Each metal is nine-coordinate in a highly distorted monocapped square antiprismatic polyhedron, produced by the three nitrogen atoms of the bound tridentate aromatic unit and by the six oxygen atoms of the three didentate hexafluoroacetylacetonates, N1 occupying the capping position (see Appendix 1). All bond distances and bond angles are standard (Tables S2–S4) and the solid-state molecular structures of [Yb$_2$(**L3**)(hfac)$_6$] and [Eu$_2$(**L4**)(hfac)$_6$] are almost superimposable, except for the interannular phenyl-benzimidazole twist angle, which increases from 54.1(1)° to 66.2(1)° (Fig. S3 and Table S5).

Irradiation into the allowed ligand-centered $^1\pi^* \leftarrow {}^1\pi$ transition of [Eu$_2$(**L4**)(hfac)$_6$] at $\bar{\nu}_{exc}$ = 28170 cm^{-1} produces an intense long-lived red emission signal, arising from **L4**→Eu(III) energy transfer followed by Eu(^{5}D$_1$) and Eu(^{5}D$_0$)-centered luminescence (Fig. S4). The emission spectrum is dominated by the hypersensitive forced electric dipolar Eu(^{5}D$_0$→^{7}F$_2$) transition centered at 16340 cm^{-1} leading to the largest global absolute quantum yields in this series (Φ_{Eu}^L=0.26(1), solid state, 293K, Table 1, entry 6).[11] Using Einstein's result for the spontaneous radiative emission rate,[12] the radiative rate constant k_r^{Eu} (Table 1, entry 2) is deduced from the I_{tot}/I_{MD} ratio, where I_{tot} is the integrated emission for the Eu(^{5}D$_0$) level (^{5}D$_0$ → ^{7}F$_J$, J = 0 – 4) and I_{MD} is the integrated intensity of the magnetic dipolar Eu(^{5}D$_0$→^{7}F$_1$) transition (Table 1, entry 1). Combined with the characteristic lifetime τ_{Eu} = 0.90(1) ms (Table 1, entry 3), we calculate Φ_{Eu}^{Eu}=0.77(1) for the intrinsic Eu-centered quantum yield (eq. 4, Table 1, entry 4), a value identical to that obtained for [Eu$_2$(**L3**)(hfac)$_6$], which implies that the gain in global quantum yields can be specifically assigned to the improved sensitization process $\eta_{sens}=\eta_{ISC}\cdot\eta_{en.tr.}^{L\rightarrow Eu}=\Phi_{Eu}^L/\Phi_{Eu}^{Eu}$=0.34(1) operating in [Eu$_2$(**L4**)(hfac)$_6$] (eq. 1, Table 1, entry 7). Given the experimental ligand-centered fluorescence lifetimes of only 30–60 ps that are measured for the [Gd$_2$(**L*k***)(hfac)$_6$] complexes (**L*k*** = **L1–L4**, Table S6), one can assume that the energy migration processes in [Eu$_2$(**L*k***)(hfac)$_6$] is well described by the exclusive contribution of the triplet state as shown in Fig. 1.[7,13] Considering that (i) the sum of the radiative and internal non-radiative conversion rate constants $k_r^F+k_{nr}^F$ controlling the relaxation of the $^1\pi^*$ excited state in the free ligand are the same in the gadolinium complex [Gd$_2$(**L4**)(hfac)$_6$] and that (ii) $k_{ISC}^{\mathbf{L4}} \ll k_{ISC}^{Gd-\mathbf{L4}}$ because of the paramagnetic and heavy atom effects generated by Gd(III),[14] the introduction of the experimental characteristic $^1\pi^*$ lifetimes measured in **L4** ($\tau_L^{\mathbf{L4}}\left({}^1\pi^*\right)$=0.25(2) ns) and in [Gd$_2$(**L4**)(hfac)$_6$] ($\tau_L^{Gd-\mathbf{L4}}\left({}^1\pi^*\right)$=0.029(6) ns, Table S6) into eq. 6 gives $k_{ISC}^{Gd-\mathbf{L4}}$=30(4) ns^{-1} (Table 1, entry 8) and $k_r^F+k_{nr}^F$=4.00(5) ns^{-1} (Table 1, entry 9), from which η_{ISC} = 0.88(15) can be deduced with eq. 2 (Table 1, entry 10).[7]

$$\frac{1}{\tau_L^{Gd-\mathbf{L}}\left({}^1\pi^*\right)}-\frac{1}{\tau_L^{\mathbf{L}}(\pi^*)}=\left(k_r^F+k_{nr}^F+k_{ISC}^{Gd-\mathbf{L}}\right)-\left(k_r^F+k_{nr}^F+k_{ISC}^{\mathbf{L}}\right)=k_{ISC}^{Gd-\mathbf{L}}-k_{ISC}^{\mathbf{L}}\approx k_{ISC}^{Gd-\mathbf{L}} \quad (6)$$

Finally, the energy transfer efficiency $\eta_{\text{en.tr.}}^{L\rightarrow\text{Eu}}=\eta_{\text{sens}}/\eta_{\text{ISC}}=0.39(6)$ and the associated rate constant $2k_{\text{en.tr.}}^{\text{Eu}}=\left[\eta_{\text{en.tr.}}^{L\rightarrow\text{Eu}}/\left(1-\eta_{\text{en.tr.}}^{L\rightarrow\text{Eu}}\right)\right]\left(k_r^P+k_{\text{nr}}^P\right)=5.7(2.1)\ \text{ms}^{-1}$ (eq. 3 with $\left(k_r^P+k_{\text{nr}}^P\right)=1/\tau_L^{\text{Gd}-\mathbf{L4}}\left({}^3\pi^*\right)=9.1(2.5)\ \text{ms}^{-1}$) calculated for [$Eu_2$(**L4**)(hfac)$_6$] (Table 1, entries 11 and 12) indicates no noticeable improvement of these parameters on changing from the difluorinated (**L3**) to the perfluorinated (**L4**) spacer, despite the 500–1000 cm^{-1} energy blue shift of the ligand-centered $^1\boldsymbol{\pi}^*$ (Fig. S5) and $^3\boldsymbol{\pi}^*$ (Fig. S6) excited states. Our simple method for dissecting the sensitization mechanism[7] shows that the gain in the global quantum yield Φ_{Eu}^L, for the complex [Eu_2(**L4**)(hfac)$_6$] as compared to [Eu_2(**L3**)(hfac)$_6$], indeed results from an optimization of the intersystem crossing process η_{ISC} (Fig. 1).

Scrutiny of the various rate constants (Tables 1 and S7) reveals that the decrease of the radiative and internal conversion rate constant $k_r^F+k_{\text{nr}}^F$ for the ligand-centered $\mathbf{L}(^1\boldsymbol{\pi}^*)$ state along the series **L2** > **L3** > **L4** acts to improve η_{ISC} (eq. 2), but it is the remarkable increase of $k_{\text{ISC}}^{\text{Ln}-\mathbf{L}}$ in [Ln_2(**L4**)(hfac)$_6$], which eventually controls the overall intersystem crossing efficiency.

The physical origin of this beneficial effect can be traced back to the golden-rule expression for radiationless transitions:[15]

$$k_{\text{ISC}}=\frac{2\pi}{\hbar}\left\langle {}^1\pi^*\left|H_{\text{SO}}\right|{}^3\pi^*\right\rangle^2\times FCWDS \quad (7)$$

where *FCWDS* is the Franck-Condon Weighted Density of States. It accounts for the density of vibrational states in the triplet and their vibrational overlap with the singlet vibrational state. A model that accounts for the thermal population of levels and uses a single quantum mode of frequency ω, is commonly associated with the Marcus-Levich-Jortner theory for electron transfer expressed in eq. 8:[16]

$$FCWDS=\frac{\exp(-S)}{\sqrt{4\pi RT}}\sum_{n=0}^{\infty}\frac{S^n}{n!}\exp\left[-\frac{(\Delta E+n\hbar\omega+\lambda)^2}{4\lambda RT}\right] \quad (8)$$

The spin-orbit coupling matrix element $\left\langle {}^1\boldsymbol{\pi}^*\left|H_{\text{SO}}\right|{}^3\boldsymbol{\pi}^*\right\rangle$ reaches a maximum for non-planar polyaromatic molecules containing heavy paramagnetic atoms in the molecular frame;[16,17] two conditions which are fulfilled by all [Eu_2(**L*k***)(hfac)$_6$] complexes described in this study. We however note that the deviation from the planarity, as measured by the interplanar phenyl-benzimidazole angles, increases along the series **L2** (25.26(4)°) < **L3** (54.1(1)°) and **L4** (66.2(1)°) in line with k_{ISC} (eq. 7 and Table 1). The Franck-Condon weighted density of states (*FCWDS*) depends on the singlet-triplet energy splitting $\Delta E=E(^1\boldsymbol{\pi}^*)-E(^3\boldsymbol{\pi}^*)$ and on the reorganization energy λ, which corresponds to the energy difference between the triplet and the singlet state at its equilibrium geometry (eq. 8).[18] In the limit of parabolic surfaces, this energy parameter, along with ΔE, provides the energy gap for $n=0$. The successive fluorination of the ligands along the series [Eu_2(**L*k***)(hfac)$_6$] (***k*** = 2–4) is known to significantly affect the frontier orbitals, hence λ and ΔE and *FCWDS* in eq. 8.[7] While a quantitative understanding of the changes in λ requires sophisticated theoretical calculations of the vibrational coupling scheme controlling the Huang-Rhys factors (***S***),[15,16] eqs (7)–(8) predict that the increasing ligand-centered energy gap ΔE observed along the series **L2** (3550 cm^{-1}) ≈ **L3** (3230 cm^{-1}) < **L4** (5200 cm^{-1}) should lower k_{ISC} and η_{ISC}. The apparent contradiction with our experimental results (Table 1, entries 8 and 10) can be resolved by including higher lying triplet states $^3\pi_{n>1}^*$ in the model; an approach used

successfully for oligothiophenes[15] and helicenes.[15b] This counter-intuitive correlation was empirically noticed for other polyaromatic chromophores, and it was suggested as a 'rule-of-thumb' that a singlet-triplet gap of $E(^1\pi^*)-E(^3\pi^*) \geq 5000\ cm^{-1}$ warrants quantitative intersystem crossing processes in Tb- and Eu-complexes.[19] Given that the singlet-triplet energy gap can be readily calculated by using DFT[7] or semi-empirical[8] methods, computations may be useful for identifying simple chemical and structural modifications that will enhance the quantum efficiency further.

In conclusion, the application of this simple method for analyzing the various contributions to Eu^{III} luminescence sensitization shows that perfluorination of the remote phenyl spacer in the rigid single-stranded dumbbell-shaped $[Eu_2(\mathbf{L4})(hfac)_6]$ oligomer optimizes both intersystem crossing efficiency and intrinsic Eu^{III} quantum yield, thus maximizing the global quantum yields in these polyaromatic rigid complexes (red histograms in Fig. 1).

Supplementary Material

Refer to Web version on PubMed Central for supplementary material.

References and Notes

1. a) Kido J, Okamoto Y. Chem Rev. 2002; 102:2357–2368. [PubMed: 12059271] b) Evans RC, Douglas P, Winscom CJ. Coord Chem Rev. 2006; 250:2093–2126.c) de Bettencourt-Dias A. Dalton Trans. 2007:2229–2241. [PubMed: 17534483] d) Binnemans K. Chem Rev. 2009; 109:4283–4374. [PubMed: 19650663] (e) Kerbellec N, Kustaryono D, Haquin V, Etienne M, Daiguebonne C, Guillou O. Inorg Chem. 2009; 48:2837–2843. [PubMed: 19265391] f) Law GL, Wong KL, Tam HL, Cheah KW, Wong WT. Inorg Chem. 2009; 48:10492–10494. [PubMed: 19842665] g) Zheng K, Zhang D, Zhao D, Liu N, Shi F, Qin W. Phys Chem Chem Phys. 2010; 12:7620–7625. [PubMed: 20544112] h) Katkova MA, Bochkarev MN. Dalton Trans. 2010; 39:6599–6612. [PubMed: 20390195] i) Eliseeva SV, Bünzli JCG. Chem Soc Rev. 2010; 39:189–227. [PubMed: 20023849] j) Farinola GM, Ragni R. Chem Soc Rev. 2011; 40:3467–3482. [PubMed: 21437308] k) Cui Y, Yue Y, Qian G, Chen B. Chem Rev. 2012; 112:1126–1162. [PubMed: 21688849] l) Liu Y, Pan M, Yang QY, Fu L, Li K, Wei SC, Su CY. Chem Mater. 2012; 24:1954–1960.m) Sava DF, Rohwer LES, Rodriguez MA, Nenoff TM. J Am Chem Soc. 2012; 134:3983–3986. [PubMed: 22339608]
2. a) Bünzli J-CG, Piguet CC. Chem Rev. 2002; 102:1897–1928. [PubMed: 12059257] b) dos Santos CMG, Harte AJ, Quinn SJ, Gunnlaugsson T. Coord Chem Rev. 2008; 252:2512–2527.c) Swavey S, Swavey R. Coord Chem Rev. 2009; 253:2627–2638.d) Faulkner S, Natrajan LS, Perry WS, Sykes D. Dalton Trans. 2009:3890–3899. [PubMed: 19440586] e) Vigato PA, Peruzzo V, Tamburini S. Coord Chem Rev. 2009; 253:1099–1201.f) Lincheneau C, Stomeo F, Comby S, Gunnlaugsson T. Aust J Chem. 2011; 64:1315–1326.
3. a) Borkovec M, Hamacek J, Piguet C. Dalton Trans. 2004:4096–4105. [PubMed: 15573160] b) Piguet C, Borkovec M, Hamacek J, Zeckert K. Coord Chem Rev. 2005; 249:705–726.
4. Dalla Favera N, Hamacek J, Borkovec M, Jeannerat D, Ercolani G, Piguet C. Inorg Chem. 2007; 46:9312–9322. [PubMed: 17915861]
5. Chen XY, Yang X, Holliday BJ. J Am Chem Soc. 2008; 130:1546–1547. [PubMed: 18183978]
6. McKenzie BM, Wojtecki RJ, Burke KA, Zhang C, Jakli A, Mather PT, Rowan SJ. Chem Mater. 2011; 23:3525–3533.
7. Lemonnier JF, Guénée L, Beuchat C, Wesolowski TA, Mukherjee P, Waldeck DH, Gogik KA, Petoud S, Piguet C. J Am Chem Soc. 2011; 133:16219–16234. [PubMed: 21882836]
8. Freire RO, Albuquerque RQ, Junior SA, Rocha GB, Mesquita ME. Chem Phys Lett. 2005; 405:123–126.
9. Yamaguchi Y, Matsubara Y, Ochi T, Wakamiya T, Yoshida ZI. J Am Chem Soc. 2008; 130:13867–13869. [PubMed: 18816053]
10. For the sake of clarity and conciseness in the discussions, the kinetic data collected for **L1**, which bears electron-donating methoxy groups, are not further considered in Fig. 1 and Table 1.

11. Global quantum yields up to 64% have been reported for polynuclear Eu(III) complexes, see Miyata K, Ohba T, Kobayashi A, Kato M, Nakanishi T, Fushimi K, Hasegawa Y. ChemPlusChem. 2012; 77:277–280.
12. $k_r^{Eu} = A(\psi_J, \psi_{J'}) = A_{MD,0} \cdot n^3 \cdot (I_{tot} / I_{MD})$ with $A_{MD,0} = 14.65\ s^{-1}$ for the magnetic dipolar Eu($^5D_0 \rightarrow {}^7F_1$) transition and a refractive index $n = 1.5$. Aebischer A, Gumy F, Bünzli J-CG. Phys Chem Chem Phys. 2009; 11:1346–1353. [PubMed: 19224035] and references therein.
13. a) Sabbatini, N.; Guardigli, M.; Manet, I. Handbook on the Physics and Chemistry of Rare Earths. Gschneidner, KA., Jr; Eyring, L., editors. Vol. 23. Elsevier Science; Amsterdam: 1996. p. 69-120.b) Faulkner S, Pope SJ, Burton-Pye BP. Appl Spectrosc Rev. 2005; 40:1–35.c) Ward MD. Coord Chem Rev. 2010; 254:2634–2642.
14. a) Tobita S, Arakawa M, Tanaka I. J Phys Chem. 1984; 88:2697–2702.b) Tobita S, Arakawa M, Tanaka I. J Phys Chem. 1985; 89:5649–5654.
15. Beljonne D, Shuai Z, Pourtois G, Brédas JL. J Phys Chem A. 2001; 105:3899–3907.and references therein. [16] Jortner J, Bixon M. Adv Chem Phys. 1999; 106:35–202.Brédas JL, Beljonne D, Coropceanu V, Cornil J. Chem Rev. 2004; 104:4971–5003. [PubMed: 15535639] Schmidt K, Brovelli S, Coropceanu V, Beljonne D, Cornil J, Bazzini C, Caronna T, Tubino R, Meinardi F, Shuai Z, Brédas JL. J Chem Phys A. 2007; 111:10490–10499.
17. Monguzzi A, Tubino R, Hoseinkhani S, Campione M, Meinardi F. Phys Chem Chem Phys. 2012; 14:4322–4332. [PubMed: 22370856]
18. For intersystem crossing, solvent effects are expected to be small and are not considered in λ. As a first approximation, λ= 1500–2000 cm^{-1} are realistic values for polyaromatic scaffolds.[15],[16]
19. Steemers FJ, Verboom W, Reinhoudt DN, van der Tol EB, Verhoeven JW. J Am Chem Soc. 1995; 117:9408–9414.

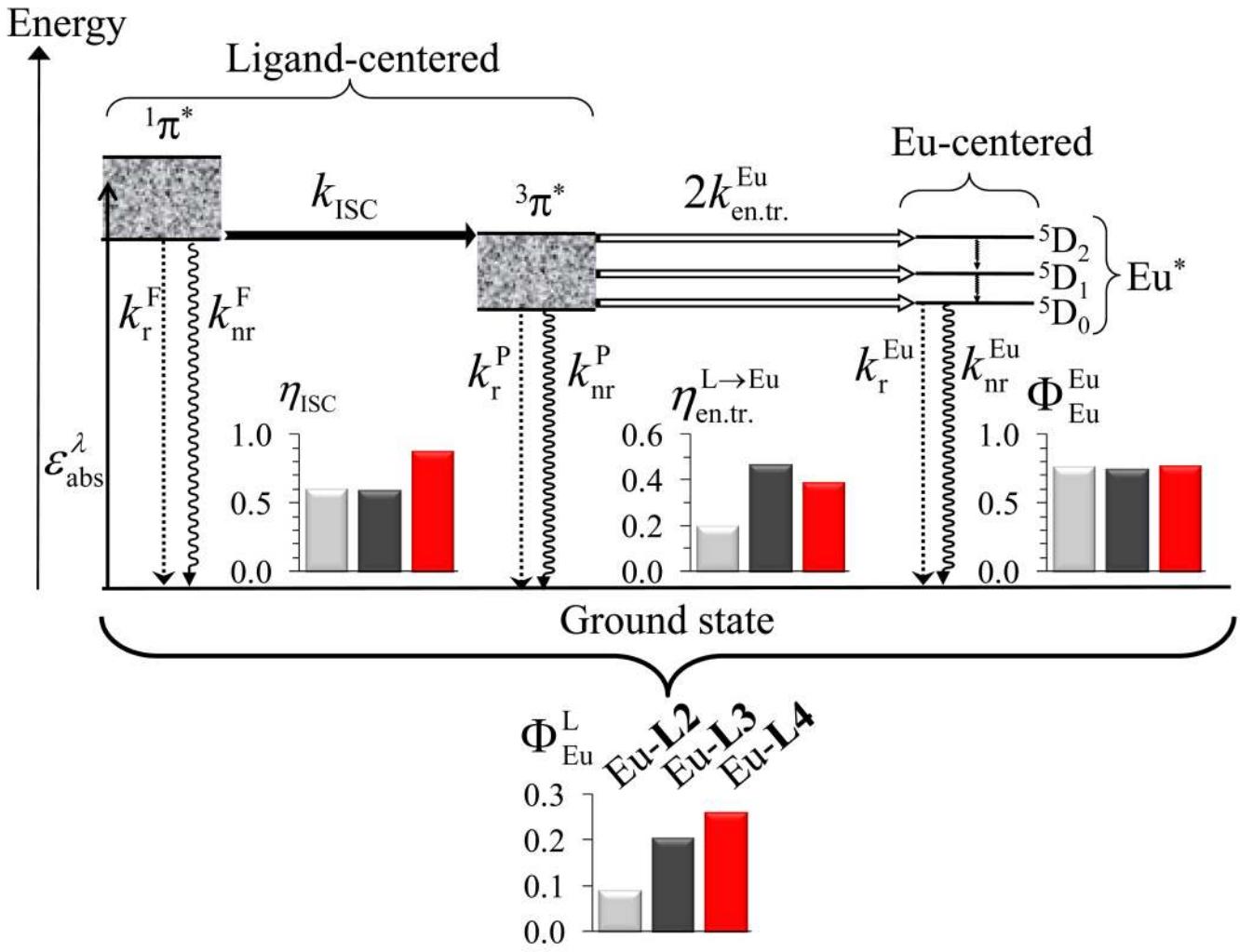

Figure 1.

This simplified Jablonski diagram for $[Eu_2(\mathbf{L}\boldsymbol{k})(hfac)_6]$ ($\boldsymbol{k}$ = 2–4) shows the ligand-centered triplet-mediated sensitization mechanism of the two Eu^{3+} ions.[10] The photophysical processes are described by the rate constants: k_r^F for ligand fluorescence, k_{nr}^F for ligand internal non-radiative conversion, k_r^P for ligand phosphorescence, k_{nr}^P for non-radiative relaxation from the ligand triplet state, k_r^{Eu} for emission of Eu^*, k_{nr}^{Eu} for nonradiative decay of Eu^*, k_{ISC} for ligand intersystem crossing, and $k_{en.tr.}^{Eu}$ for the ligand-to-metal energy transfer. Efficiencies of intersystem crossing (η_{ISC}), energy transfer ($\eta_{en.tr.}^{L\rightarrow Eu}$), intrinsic quantum yield (Φ_{Eu}^{Eu}), and quantum yield (Φ_{Eu}^{L}) for the global ligand-mediated sensitization of Eu^{III} in $[Eu_2(\mathbf{L}\boldsymbol{k})(hfac)_6]$ (solid-state, 293 K).

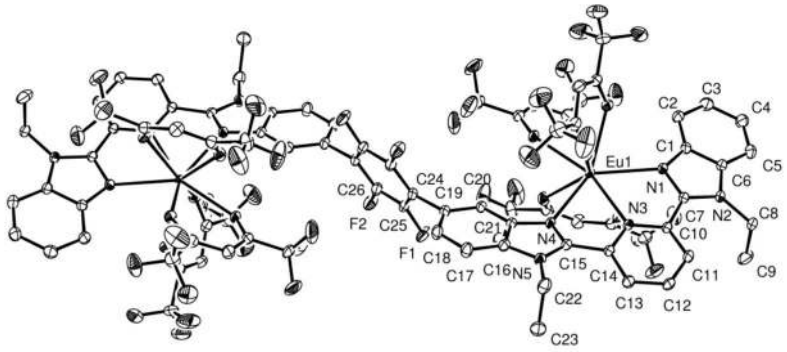

Figure 2.

Perspective view of the molecular structure of $[Eu_2(\mathbf{L4})(hfac)_6]$ as obtained from X-ray diffraction with numbering scheme. Thermal ellipsoids are represented at the 30% probability level and hydrogen atoms are omitted for clarity.

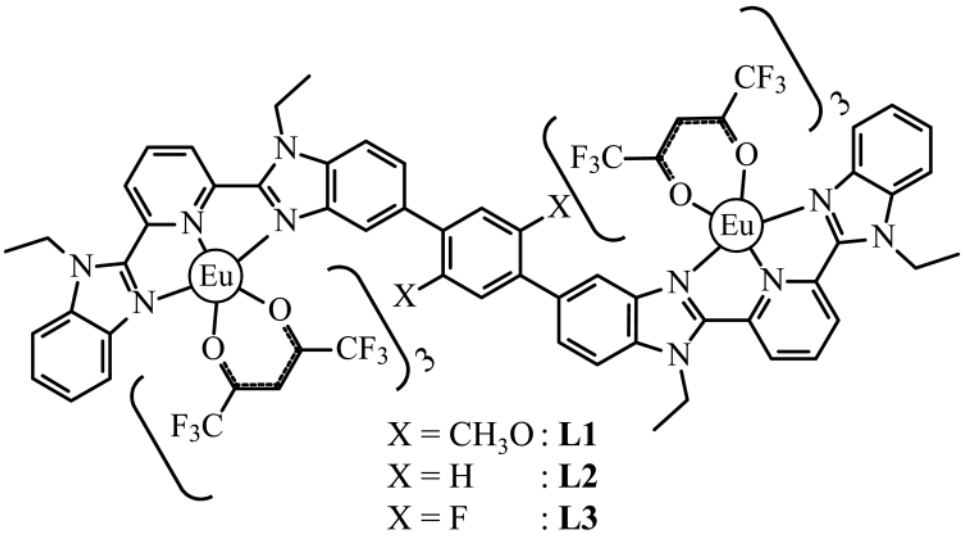

Scheme 1.
Chemical structures of complexes $[Eu_2(\mathbf{L}\boldsymbol{k})(hfac)_6]$

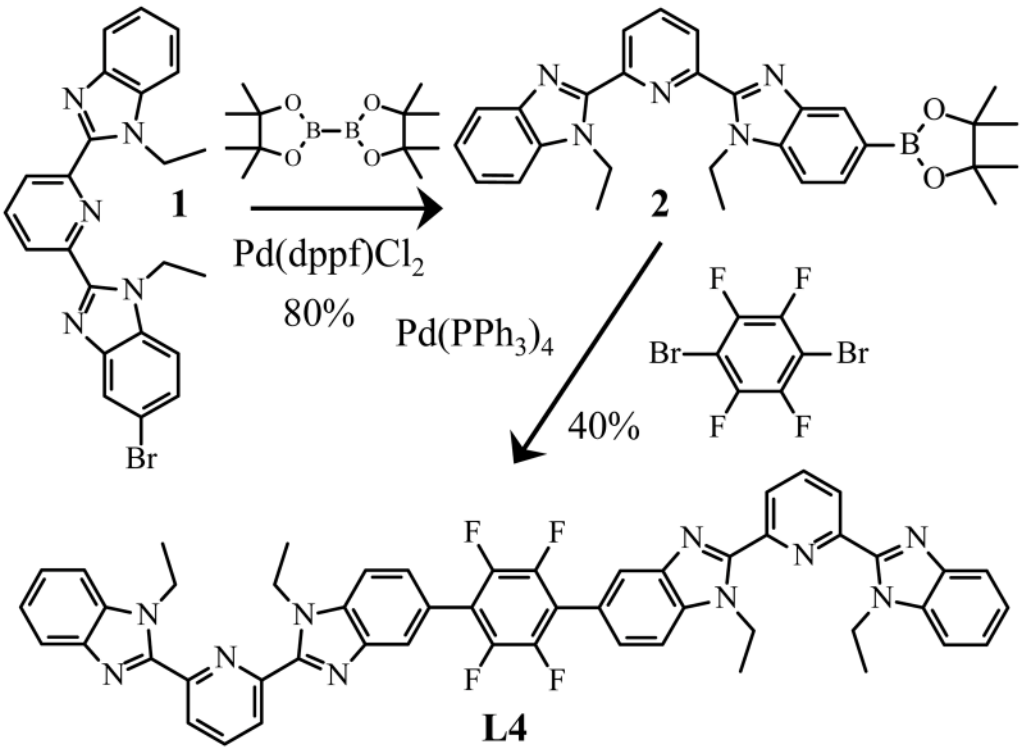

Scheme 2.
Synthesis of the perfluorinated ligand **L4**.

Table 1

Experimental global (Φ_{Eu}^{L}) and intrinsic (Φ_{Eu}^{Eu}) quantum yields, luminescence lifetimes (τ_{Eu}) and calculated energy migration efficiencies (η_{ISC}, $\eta_{en.tr.}^{L\rightarrow Eu}$) and rate constants (k_r^{Eu}, k_{nr}^{Eu}, $k_{en.tr.}^{Eu}$, $k_r^P+k_{nr}^P$, k_{ISC}) for [Eu_2(**L*k***)(hfac)$_6$] in the solid state at 293 K (k = 2–4).[10]

Compound	**[Eu_2(L2)(hfac)$_6$]**	**[Eu_2(L3)(hfac)$_6$]**	**[Eu_2(L4)(hfac)$_6$]**
Eu-centered luminescence			
I_{tot}/I_{MD}	17.5(3)	18.2(3)	17.2(2)
k_r^{Eu}/ms^{-1}	0.86(2)	0.90(2)	0.85(1)
τ_{Eu}/ms	0.88(4)	0.83(15)	0.90(1)
Φ_{Eu}^{Eu}	0.76(4)	0.75(1)	0.77(1)
k_{nr}^{Eu}/ms^{-1}	0.21(1)	0.23(4)	0.200(4)
Global quantum yield and sensitization efficiency			
Φ_{Eu}^{L}	0.092(3)	0.206(7)	0.26(1)
$\eta_{ISC}\cdot\eta_{en.tr.}^{L\rightarrow Eu}$	0.122(7)	0.28(5)	0.34(1)
Energy migration and associated rate constants			
$k_{ISC}^{Gd\text{–}L}/ns^{-1}$	10.0(6)	9(2)	30(4)
$k_r^F+k_{nr}^F/ns^{-1}$	6.71(5)	6.25(3)	4.00(5)
η_{ISC}	0.60(3)	0.59(12)	0.88(15)
$\eta_{en.tr.}^{L\rightarrow Eu}$	0.20(2)	0.47(14)	0.39(6)
$2k_{en.tr.}^{Eu}/ms^{-1}$	2.1(3)	5.5(2.3)	5.7(2.1)
$k_r^P+k_{nr}^P/ms^{-1}$	8.1(5)	6.3(8)	9.1(2.5)
Reference	[7]	[7]	This work